A Model of Magnetic Field and Mass Flows in Dark Filaments

by

Yutaka Uchida
Tokyo Astronomical Observatory
University of Tokyo, Mitaka, Tokyo

Abstract

A model of magnetic field in the dark filament having a "neutral sheet" in $B_\perp$ (the field component perpendicular to the polarity reversal line in the photosphere) is obtained by solving the equation for the magnetostatic equilibrium. The apprearance of the "neutral sheet" structure is due to the assumed (line-) quadrupole component in the photospheric magnetic field distribution, and, from the standpoint of view of the neutral sheet hypothesis of flares, it is favorable in explaining the fact that the dark-filament disappearance is connected to the occurrence of flares. Further,possible mass-flow is examined in the derived magnetic field configuration in order to explain the steady supply of mass for the downflow across the height of the prominence. It turns out that there is a steady Bernoulli flow solution which first increases its velocity towards the top of the loop and then diminishes its velocity on approaching the "neutral sheet" region, explaing the slow downflow observed in the prominences.

1. Introduction

A dark filament is an elongated, thin partition-like object (length $\simeq$ (1 - 2) x 10^5 km, width $\simeq$ a few x 10^3 km, height$\simeq$ (2 - 5) x 10^4 km) lying over the polarity reversal line of the photospheric magnetic field (McIntosh 1972). When seen from above, it is consisted of thin threads along the length of the structure with centipede-leg type features on both sides of it. Thin threads are also observed when seen on the limb (or seen from sideward) with a continuous downflow along them (Engvold 1976).

A dark filament is thus considered to be a structure due to magnetic field which suspends the material against gravity, and many theoretical models for the magnetoplasma equilibrium have been proposed to explain the observed characteristic features of it (Bhatnager et al 1951, Dungey 1953, Brown 1958, and so on. See Tandberg-Hanssen 1974 for review). One of the most widely discussed modelds among them is Kippenhahn and Schluter's model

(1957). It is a model in which the mass is suspended by a sagged magnetic field lines and a thin partition-like structure is considered as the locus of the lowest points on the similarly sagged group of lines of force at which low temperature mass is sedimented with a short scaleheight.

Kippenhahn-Schluter model, however, deals with sagged field lines locally, and actually the sagging is due to the specification of the boundary value of B_z/B_x . In actuality, if we consider that the lines of force above the polarity reversal line of the photospheric magnetic field is convex, there is no way for the mass pile-up to start because it is not possible to suspend the mass on the top of the convex field lines. The production of the dip, on the other hand will be appreciable only after the amount of the loaded mass at the top of the loop reaches an appreciable amount. In other words, the mass slides down and can not stay at the top to sag the lines of force if it is initially convex. Another difficulty with K-S model may be the fact that there is a steady downward mass flow observed across the height of the dark filament, but K-S model does not have a drainage installed in it. The mass down-flow suggests that the mass of the dark filament is replaced in every several hours, and that there should be a supply of the mass either from the surrounding corona, or from the chromosphere by some special means. The former, however, is difficult because it means a mass flow across the field lines as long as we consider the thread-like structure as representing the field lines. In the latter line, the mechanism proposed by Meyer and Schmidt (1968) for the flow in coronal loop was applied to the present problem of the mass supply to the dark filament by Pickelner (1971). Pickelner's model, however, has no drainage again and does not explain the down-flow in the steady state.

Our model to be discussed here explains the observational characteristic features of the dark filament described at the begining of this section, as well as its relation to the polarity-reversal lines, and gives naturally an explanation for the flows down across the prominences (dark filament seen on the limb). In section 2 we describe the solution for the magnetoplasma equilibrium (Uchida and Jockers 1977, 1981), and in section 3 we discuss the result of the calculation of the flow induced in the structure by syphon mechanism (summary of the work done by Uchida and Tsuneta 1978, 1981). Discussions are given in section 4.

2. A Solution for the Magnetoplasma Equilibrium

Uchida and Jockers' (1977) solved the equation for the equilibrium of magnetoplasma under constant gravity,

$$\frac{1}{c}\, j \times B - \nabla p + \rho g = 0 \,, \quad j = \frac{c}{4\pi} \mathrm{rot}\, B \tag{1}$$

for quasi-three dimensional configuration (the field has three components but does not depend on one coordinate, say, y along the polarity-reversal line in the photospheric magnetic field). In this case, B is expressible by two variables, φ and $B_{\parallel}(\parallel y)$ as

$$B = \left(\frac{\partial \varphi}{\partial z} \,,\; B_{\parallel} \,,\; -\frac{\partial \varphi}{\partial x} \right) \tag{2}$$

and it can be shown that the problem reduces to solving

$$\nabla_{\perp}^2 \varphi + \frac{1}{2} \frac{d}{d\varphi} \left\{ B_{\parallel}^2(\varphi) + 8\pi p_0(\varphi) e^{-z/z_s} \right\} = 0 \tag{3}$$

where $\nabla_{\perp}^2 \equiv \partial^2/\partial x^2 + \partial^2/\partial z^2$, $z_s \equiv RT/g$ and $B_{\parallel}$ is required to be the function of φ alone from the force balance along y-axis, and p_0 is the pressure at z = 0 which may be the function of φ. The pressure assigned according to the boundary condition at the base now distributes hydrostatically along the magnetic tubes of force protruding in the corona.

In order to avoid the difficulty of convex field lines in supporting the cold mass loaded upon them, Uchida and Jockers introduced a quadrupolar component in the distribution of photospheric magnetic field. This introduces the possibility for a "neutral sheet" (in $B_{\perp}$) to appear right above the polarity reversal line and also gives rise to a dip to the otherwise convex field pattern. It is rather surprising that the neutral sheet structure has never been considered in the context of the dark filament models while the disappearance of the dark filament is known to be related to the occurrence of flares and the neutral sheet hypothesis has been discussed as a likely mechanism of flares during the last twenty years. Our dark filament model is the one which is intrinsically related to a "neutral sheet" (in and $B_{\perp}$) and its relation to flares is discussed in Uchida and Sakurai (1980) and in Uchida (1981). As for the distribution of $B_{\parallel}$ and p_0 , we assume

$$B_{\parallel} = B_{\parallel 0} \exp\left\{ -\frac{(\varphi - \varphi_c)^2}{\sigma_{B_{\parallel}}^2} \right\} \tag{4}$$

and

$$p_0 = p_{0c} + p_{0c} \exp\left\{ - \frac{(\varphi - \varphi_c)^2}{\sigma_p^2} \right\} \qquad (5)$$

as an example in the calculation.

We solve equation (3) by using an extended version of Jockers' code with Marder and Weitzner's relaxation scheme, which was used for the force-free field case (Jockers 1978). The result is shown in Figure 1 and the central part of it having the centipede-leg like feature is shown in Figure 2. It is seen in Figure 1 that our model indeed has a thin vertical "neutral sheet" of $B_\perp$ right above the polarity reversal line of the photospheric magnetic field, and the effect of relatively small $B_\parallel$, dominates in this sheet of vanishing $B_\perp$, and field lines shows a strong tendency of aligning along the y-axis in the sheet. The lines of force, all of which would be convex without the quadrupolar component in the photospheric field distribution, are now deformed to have sagged part as well as sheet structure, due to the introduction of the quadrupolar distribution of the field near the polarity reversal line.

3. Supply of the Mass by Steady Flow

Although the solution shown above is that for a static equilibrium and no mass-flow is installed in it, we may discuss the mass-flow in the configuration without deforming it too much, since $\rho v^2/2 \ll B^2/8\pi$, and $\mathcal{R}\rho T \ll B^2/8\pi$ even in the sheet. Thus, we consider the magnetic tubes of force as fixed pipes and write hydrodynamic equations in them. We have for steady flows,

$$\frac{1}{A}\frac{d}{ds}(AB) = 0 \qquad (6)$$

$$\frac{1}{A}\frac{d}{ds}(A\rho u) = 0 \qquad (7)$$

$$\rho \frac{du}{ds} = -\frac{dp}{ds} - \rho \frac{GM}{r^2}\frac{dr}{ds} \qquad (8)$$

$$\frac{1}{A}\frac{d}{ds}\left[A\rho u\left(\frac{u^2}{2} - \frac{GM}{r} + \frac{5}{2}\mathcal{R}T\right) - AK\frac{dT}{ds}\right] = Q - \rho^2\Phi \qquad (9)$$

where A(s) is the crosssectional area of tubes of force, and s is the length measured along them. A(s) is related to the magnetic field strength, B(s), as AB = const, and is given from the model

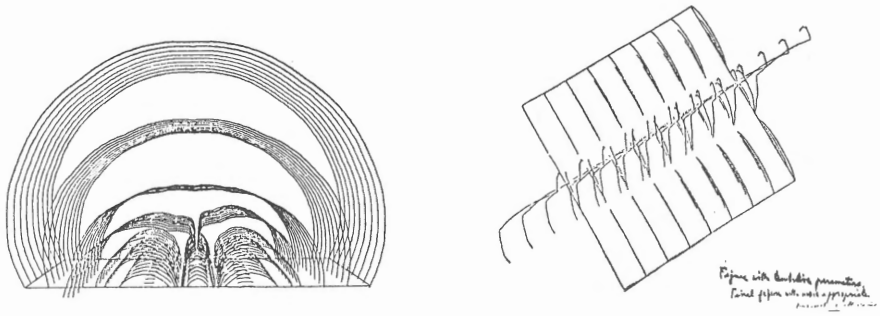

Fig. 1. A solution for the magnetic field in dark filaments. Quadrupolar component in the photospheric magnetic field distribution introduces a "neutral sheet" (neutral sheet in $B_\perp$) above the central polarity reversal line.

Fig. 2. A part of the structure of the field configuration of Figure 1. Field lines are stretched along the neutral sheet of $B_\perp$, because even comparatively weak $B_{//}$ dominates in the sheet where $B_\perp = 0$.

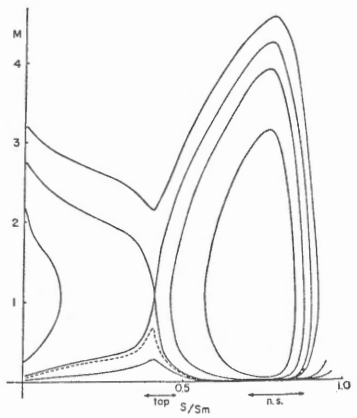

Fig. 3. s-M diagram for the steady polytropic flow. The solution fulifilling the condition that the flow slows down and condenses on approaching the sheet region is the one shown in dotted curve, staying subsonic all the way. The flow is accelerated and has a maximum velocity near the top of the loop and then diminishes its velocity.

in section 2. Other notations are as usual.

If we first assume a polytropic gas for simplicity, equations(9) is replaced by $p\rho^{-\alpha}$ =const, and equations (7) and (8) are integrated parallel to the solar wind case (cf. Kopp and Holtzer 1976) to give

$$M^{\frac{4}{\alpha+1}} + \frac{2}{(\alpha-1)M^{2\frac{\alpha-1}{\alpha+1}}} = \left\{ M_0^{\frac{4}{\alpha+1}} + \frac{2}{(\alpha-1)M^{2\frac{\alpha-1}{\alpha+1}}} \right\} \frac{f(s)}{f_0} \qquad (10)$$

$$f(s) = \left\{ A(s) \right\}^{2\frac{\alpha-1}{\alpha+1}} \frac{E' - gh(s)}{E'} \qquad (11)$$

$$E' = \frac{u^2}{2} + \frac{5}{2}\mathcal{R}T \qquad (12)$$

The s-M diagram for a typical tube of force passing the sheet is shown in Figure 3.

It shows that the diagram is very much different from that of the solar wind case due to the area-variation effect and to the effect of the change in the effective gravity along the path, even changing signs with respect to the flow direction. Appropriate solution for our case is in the subsonic branch all the way, and the velocity change along the path, increasing near the highest part of the path and decreasing again in the sheet region, is favorable in explaining the observation.

The assumption of polytropic gas is equivalent to assuming heat sources and sinks distributed along the path in a very artificial way, and also has a restriction that the range of the allowed variation of T, for example, is not wide enough to cover the variation of the temperature expected in reality. Thus we have to recouse to numerical integration of equations (6) through (9) by adopting appropriate expression for $\mathcal{Q}$ and Φ . Figure 4 is the s-M diagram corresponding to Figure 3, and Figures 5 through 7 are u, ρ and T as functions of s . Now, for example, the temperature can fall to lower value with a higher value of density which can not be attained in the polytropic case due to the restriction of polytropic relation.

Interpretation of the results of the calculation may be as follows. From these figures, it is seen that the flow deviates very much from the polytropic case when the radiative cooling becomes effective. The temperatrure falls very much more than what the polytropic relation allows, and the velocity decreases also due to the increase in the density. All these take place when the flow approaches the sheet region. For a given tube of

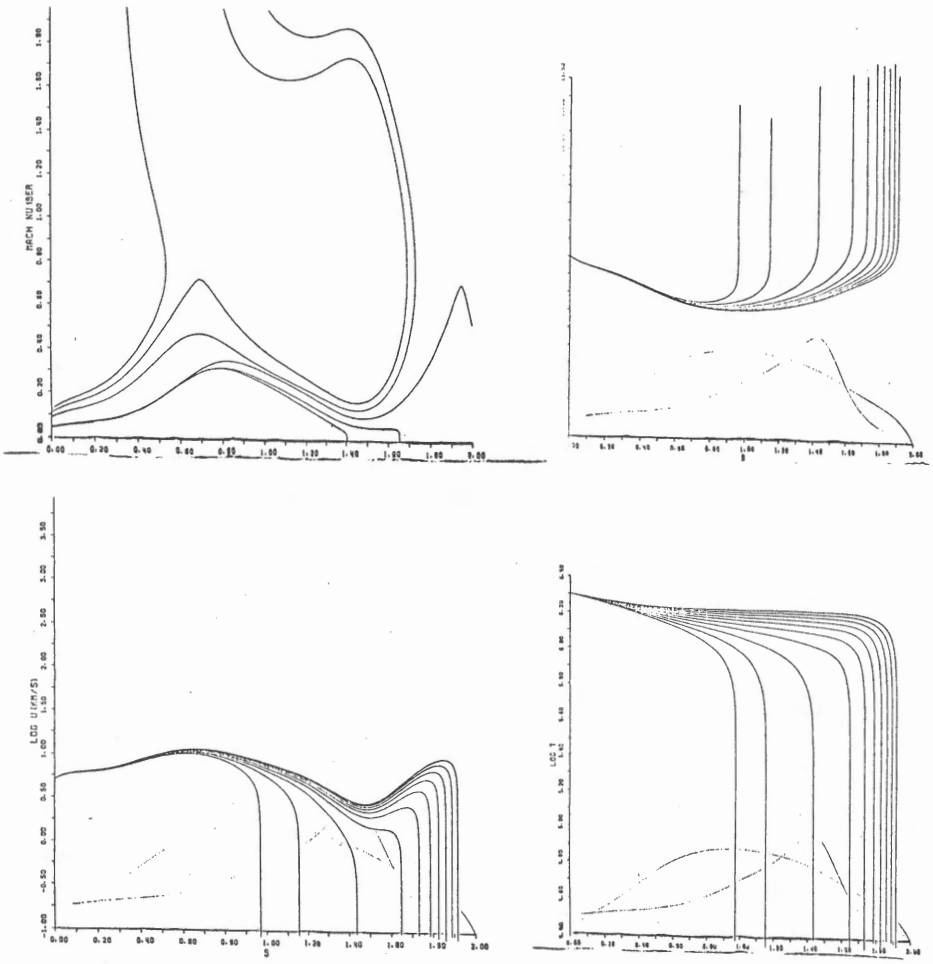

Fig. 4. Steady flow under more realistic conditions of energy exchange. s-M diagram corresponding to Figure 3.
Fig. 5. The velocity variation along the path.
Fig. 6. The density variation along the path.
Fig. 7. The temperature variation along the path.

force, the condition at the starting point (eg , the velocity, when the temperature and the density there are given) is selected out as in the Parker-flow of the solar wind case. The kinetic energy and enthalpy fluxes converts into each other, and if we put too large an inflow, the temperature of the gas gets too high when the kinetic energy is converted into enthalpy before radiative cooling region in and near the sheet is reached, because the excess heat is conducted backward to the starting point which is taken to be in the low corona at the outer footpoint of the flux tube.

Our conclusion is that there is a condition in the subsonic branch in which the flow velocity first rises to a considerable value but slows down again nicely towards the sheet region with high condensation rate and with a decreased temperature as low as 10^4 K, and reproduces the observed slow down-flow of the cool prominence material.

4. Summary and Discussion

Details of the calculation of the equilibrium field configuration and flows in it, together with interpretations of the results of calculations, may be found elsewhere as indicated. Here we summarize them as follows :

We propose a possible equilibrium configuration of magnetoplasma, which has a neutral sheet in $B_\perp$ (with $B_\parallel$ field lying in the sheet) caused by the quadrupolar component in the distribution of the photospheric field, as a possible field configuration in dark filaments. Morphological properties of the dark filament (thin partition-like structure over the polarity reversal line with fine threads along it and centipede-leg like feature on both sides) is pretty well reproduced. We consider the possibility of driving a steady flow in it by syphon mechanism (such a flow can take place without disturbing the equilibrium configuration too much). It is not possible for this mechanism to operate between two equivalent points of a symmetrical loop, but in the present case, the flow is caused between the outer and inner footpoints of the field lines on one side of the sheet, and the thermal expansion flow is driven by the pressure difference between the corona above the outer footpoint and the cooled prominence material which is drained down to the inner footpoint. In our picture, therefore, the mass down-flow observed in prominences is supplied from the low corona on the onter foot of the loop. The mass-flow passes through the top part of the loop with the highest velocity and then, on approaching the sheet region, it condenses through the radiative cooling and its velocity diminishes to reproduce the observed slow down-flow. Thus, it seems that our picture may provide a possible model for dark filaments.

References

Bhatnagar,P.L.,Krook,M ,and Menzel,D.H ,1951,in Report of Conf. on Dynamics of Ionized Media, Univ. College, London.

Brown,A.,1958,Astrophys.J.,128,646.

Dungey,J.W.,1953 Month. Not. Roy. Astron. Soc.,113,180.

Engvold,O.,1976, Solar Phys. 49, 283.

Jockers,K.,1978, Solar Phys. 56, 37.

Kippenhahn,R.,and Schluter,A.,1957,Zeit.Astrophys,43,36,

McIntosh,P.S. ,1972 in Solar Activity Observations and Predictions, eds. McIntosh and Dryer (MIT Press).

Meyer,F.,and Schmidt,H.U.,1968,in IAU Symp.No 35, Structure and Development of Solar Active Region, ed.,K.O.,Kipenhener (D.Reidel).

Pickelner,S.A.,1971,Solar Phys.17,44.

Uchida,Y. and Jockers,K.,1977,Abstract, Ann.Meeting of the Astronomical Society of Japan.

Uchida,Y. And Jockers,K.,1981, in preparation.

Uchida,Y.,and Sakurai,T.,1980, in Solar Flares, ed. Sturrock (Univ. Colorado Press).

Uchida,Y.,and Tsuneta,S.,1979, Abstract, Ann.Meeting of the Astronimcal Society of Japan.

Uchida,Y.,and Tsuneta,S.,1981,in preparation.

Uchida,Y.,1981,IAU Symp. No91, Solar and Interplanetary Dynamics, ed. Tandberg-Hanssen and Dryer (D.Reidel).

Tnadberg-Hanssen,E.,1974, Solar Promineces,(D.Reidel).